Pd/CeO_2 catalysts prepared by solvent free mechanochemical route in the exhaust gas aftertreatment of natural gas fueled vehicles

Maila Danielis[1], Sara Colussi[1], Jordi Llorca[2], Rachael Harrington Dolan[3], Giovanni Cavataio[3], Alessandro Trovarelli[1]

[1] Dipartimento Politecnico, Università di Udine, and INSTM, via del Cotonificio 108, 33100 Udine, Italy

[2] Institute of Energy Technologies, Department of Chemical Engineering and Barcelona Research Center in Multiscale Science and Engineering, Universitat Politècnica de Catalunya, EEBE, Eduard Maristany 10-14, 08019 Barcelona, Spain

[3] Research and Innovation Center, Ford Motor Company, 2101 Village Road, Mail Drop 3179, Dearborn MI 48124 USA

Keywords: methane combustion, methane steam reforming, Ceria, mechanochemistry, TWC

ABSTRACT

The increasing diffusion of alternative mobility solutions, ranging from electric technologies to natural gas fueled vehicles (NGVs), has led to a progressive life-cycle analysis approach of their environmental impact in terms of greenhouse gases (GHGs) emissions. This new approach prompted a careful design of the NGVs catalytic aftertreatment system in order to minimize the catalytic converter carbon footprint as well as the unburned methane emissions at tailpipe. Here, a series of Pd/CeO_2 methane oxidation catalysts were prepared by an environmentally friendly solvent-free method and compared to the commercial wet-synthesized state-of-the-art catalysts. Their application in NGVs aftertreatment systems was evaluated by testing powder catalysts and coated monolith cores for CH_4 oxidation and steam reforming, which are the main methane abatement reactions occurring in a three-way catalyst (TWC) under lean and rich conditions, respectively. Pd/CeO_2 catalysts prepared by mechano-chemical synthesis initially displayed superior activity to their commercial counterpart, especially under lean oxidation conditions, but appeared less resistant to the industrial aging process after core washcoating. Lambda sweep experiments carried out under full gas composition proved that, despite needing further optimization in the washcoating and aging processes, the developed mild milling synthesis procedure is a viable way for the production of Pd/CeO_2 based catalysts for natural gas TWCs.

1. INTRODUCTION

In the latest decades, natural gas has emerged as one of the most appealing and competitive alternative fuel due to its ready availability, lower price compared to liquid fuels, and technological maturity.[1–4] Its chemical composition, comprising mostly methane and some short-chain hydrocarbons (C_2H_6, C_3H_8 and C_4H_{10}, up to 20%),[5] allows for a significant reduction of CO_2 emissions due to its low C:H ratio and the possible integration with biogas.[5,6] In addition, the higher flame stability and lower flame temperature of CH_4 reduce the amount of NO_x formed in the engine,[1,7] making their abatement to increasingly stringent legislation limits easier and, consequently, cheaper. Nevertheless, methane has a global warming potential that is 25 times higher than CO_2 and its leakage needs to be carefully controlled.[8] For NGVs, unburned CH_4 slips to the atmosphere during the whole life cycle of natural gas, from the extraction and distribution steps (Well-to-Tank, WTT) to vehicle use (Tank-to-Wheel, TTW),[9] by evaporation from the fuel tank or by release of residual unburned fuel from the exhaust gases.[3,10] With a focus on the latter, catalysts manufacturers are currently challenged to design novel catalytic converters ensuring compliance with the emission limit legislation, possibly reducing the expensive noble metal loading and finding more sustainable production technologies, as expected by the core issues of the 2030 EU objectives on sustainable processes and the UN sustainable development goals.[11]

A key issue for the design of catalytic converters is their durability, as legislation emission limits are imposed over a certain minimum mileage (120’000-500’000 km) depending on vehicle category.[12] This is especially critical for NGVs aftertreatment systems, where the high amount of steam produced by CH_4 combustion (ca. 10-15%) acts as a strong inhibitor of methane oxidation catalysts.[13–15] The most common technology currently employed is a Pd-based three-way catalyst (TWC), in which simultaneous oxidation of CO and CH_4 and reduction of NO_x are achieved by

working around the stoichiometric air-to-fuel ratio value $(A/F)_s$.[16–18] The working operation in a strict lambda window is controlled by an O_2 sensor at the catalyst outlet.[17] Due to the feedback control system, the metal-metal oxide catalyst experiences brief lean-rich oscillations going from oxidative to reducing atmosphere very quickly.[19–21] The transient and cycling behavior further affects catalytic performance by modifying the palladium active sites or by enabling methane abatement via reforming reactions, as such it was widely investigated in the literature.[21–27]

Another key issue is the "cold-start" release of methane, *i.e.* unburned methane released in the first 1-3 minutes following engine ignition when the flue gases are too cold for efficient methane conversion. Currently, it accounts for the major contribution to CH_4 release in optimized aftertreatment systems[18] since the stable nature of CH_4 molecule (C-H bond energy = 439 kJ/mol) hinders its low temperature abatement.[5] Several approaches have been considered to reduce its ignition delay, including innovative design of the reactor setup for faster heating[28] and optimization of the Pd active phase for CH_4 activation at lower temperature.[29,30] This is often accomplished by tuning the optimal amount of Pd^{x+} surface species ($0 \leq x \leq 4$) which are stabilized on the surface and subsurface region based on reaction conditions, surface dopants and support type.[31–34]

We previously reported a novel solvent-free mechano-chemical route for the synthesis of highly active methane oxidation Pd/CeO_2 catalysts starting from either metallic Pd nanopowders or Pd salts.[35,36] The developed synthesis procedure resulted in catalytic materials with a peculiar core-shell morphology, displaying enhanced methane oxidation activity at low and high temperature and improved stability in the presence of excess steam. The enhanced reactivity is strongly dependent on the synthesis approach[37] and can be ascribed to highly dispersed Pd/PdO species in close interaction with ceria, embedded in an amorphous shell structure that likely contributes to

their stability throughout reaction.[38] Moreover, the mechanical milling procedure removes the use of solvents from the Pd loading step, avoiding the subsequent drying and calcination stages required by the conventional incipient wetness impregnation technique and reducing the time and energy needed for production.

Here, we investigate the application of Pd/CeO_2 dry milled catalysts in typical exhaust methane abatement conditions, namely methane oxidation and methane steam reforming reaction, both as powder catalysts and as washcoated monoliths. Their catalytic performance is evaluated in comparison with commercial Pd/CeO_2 samples and fully formulated TWC, and their durability is tested through fast aging procedures.

2. EXPERIMENTAL SECTION

2.1. Catalysts synthesis. Pd/CeO_2 catalysts with 1 and 4 wt.% Pd loadings were prepared on commercial high surface area ceria, calcined in the range 873 K - 1473 K prior to metal deposition. Samples were prepared by dry mechano-chemical synthesis using solid $Pd(OAc)_2$ precursor (Sigma Aldrich, 99.99%) and by standard incipient wetness impregnation using an aqueous $Pd(NO_3)_2$ solution (10 wt.% in 10 wt.% nitric acid, Sigma Aldrich, 99.999%), following established synthesis procedures.[38] Briefly, for the milling synthesis appropriate amounts of $Pd(OAc)_2$ and pre-calcined CeO_2 solid powders were loaded in a 15 mL ZrO_2 jar with a ZrO_2 grinding ball (10mm diameter, 10g weight) and milled at 15 Hz for 20 minutes using a Fritsch Pulverisette 23 Minimill; two subsequent 10-minute steps were carried out to avoid agglomeration. For the IW synthesis, an appropriate amount of $Pd(NO_3)_2$ solution in HNO_3 was used to wet the ceria powders, which were dried at 373 K for 15 hours before calcination at 873 or 1173 K

(corresponding to the support oxide calcination temperature). Prepared samples are denoted as *x*PdCe(T)M and *x*PdCe(T)IW, respectively, *x* being the nominal Pd loading in weight and (T) the calcination temperature of the support oxide. A reference sample was prepared by incipient wetness impregnation on commercial Al_2O_3 (Sasol Puralox TH100/150), calcined at 873 K prior to Pd loading (4PdAl873IW). The catalytic activity of a commercial fully formulated TWC (FF-TWC), containing both Pd and Rh, was also evaluated. The fully formulated TWC has a total PGM level of 200 g/ft^3 with ratio (0/10/1), corresponding to approximately 4wt.%Pd in the washcoat (ca. 3 grams per cubic inch washcoat loading) and a relatively large amount of Rh (10% of total PGM, 20 g/ft^3 Rh).

To prepare the necessary amount of catalyst for the washcoating process, the synthesis of a 4PdCe1473M milled sample was scaled up in a Pulverisette 6 planetary ball mill, using a 250 ml ZrO_2 jar filled with two ZrO_2 grinding balls of 20 mm diameter, each weighting ca. 24 g. 9.60 g of CeO_2(1473) and 0.844 g of Palladium acetate powders were loaded in the grinding bowl and milled for 10 minutes at 100 rpm. The scale up was designed to mimic the same operating conditions employed in the Pulverisette 23 Minimill: the low operating rpm ensures mostly shear stresses are developed during milling, while the Ball-to-Powder weight Ratio (BPR) was decreased from 10 to 5 to account for the increased number of impacts and released energy caused by the use of two grinding balls instead of a single one.

Washcoated catalyst monoliths were prepared by depositing the prepared powder catalysts on bare cordierite cores with 900/2 cells per square inch (CPSI) and measuring 0.70" D x 1.0" L. The target loading for the active catalyst powder was 3.0 grams per cubic inch (gci). To ensure good washcoat adhesion, the cordierite cores were first pre-treated with a boehmite solution (20wt.% solids/80wt.% deionized water) to deposit a thin layer of alumina (0.25 gci). The cores were

completely immersed in the boehmite solution, treated with an air-knife to blow out excess solution, dried 1 hour at 423 K, and finally calcined in air for 1 hour at 873 K. Next, the same procedure was implemented for washcoating the active catalyst. The active catalyst solution consisted of 19 wt.% catalyst, 1 wt.% boehmite, and 80 wt.% deionized water. To achieve the target 3.0 gci active catalyst loading, up to 10 cycles of the procedure was required.

2.2. Catalysts characterization. Characterization of the materials was carried out by means of BET surface area measurements, ICP-mass elemental analysis, X-ray diffractometry, high-resolution transmission electron microscopy (HRTEM) and temperature programmed oxidation (TPO) tests. BET surface area was measured with a Micrometrics Tristar Porosimeter by analyzing N_2 adsorption isotherms at 77 K. ICP-mass elemental analysis was used to measure the actual palladium loading of prepared samples. XRD analysis was performed in a Philips X'Pert diffractrometer equipped with an X'Celerator detector using Ni-filtered Cu Kα radiation ($\lambda = 1.542$ Å) recording data in the 20-100° 2θ range (0.02° step size, 40 s counting time per step). Microstructural characterization by high-resolution transmission electron microscopy (HRTEM) was carried out at 200 kV with a JEOL JEM-2010F electron microscope equipped with a field emission gun. TPO analysis was performed to follow the oxygen uptake and release of prepared samples. 150 mg of powder catalyst, placed in a quartz reactor (ID 6mm) on top of a quartz wool bed, was exposed to a flowing mixture (60 ml/min) containing 2 vol% O_2 in N_2. The temperature was increased at 10 K/min from RT to 1273 K, performing three heating/cooling cycles to reach stable behavior; the oxygen concentration was monitored continuously with an on line ABB Magnos 106 paramagnetic analyzer.

2.3. Powder samples activity tests. Evaluation of catalytic activity was performed at low and high space velocity experimental conditions with increasing gas mixture complexity. Preliminary

methane oxidation tests were performed on all samples in a lab-scale microreactor, loading 120 mg of catalytic sample in a quartz tubular reactor (ID 6mm) under 180 ml/min of a dry lean gas mixture (0.5% CH_4, 2% O_2, He to balance) to reach a final GHSV of ca. 180'000 h^{-1}.[38] Light-off profiles were recorded from room temperature to 1173 K with a heating rate of 10 K/min; three light-off cycle were normally carried out on one sample and the second cycle was taken as representative of the catalytic behavior. Reactants and products were continuously monitored with an on line ABB Uras 14 – Magnos 106 gas analyzer, and the temperature was measured with a K-type thermocouple on top of the catalytic bed. Another set of tests in methane oxidation and steam reforming was carried out on selected samples using pressed and sieved catalyst powders, diluting 500 mg of sample with 500 mg of ground up cordierite loaded in a 0.50" OD quartz reactor tube between two beds of quartz wool. The FF-TWC coated core was ground to coarse powder before loading in the quartz reactor. For methane oxidation tests, 2 L/min of reaction mixture (0.1% CH_4, 1% O_2, 5% H_2O, 5% CO_2 in N_2, λ=1.03) were introduced and the sample was heated from 373 K to 1173 K for three consecutive heating/cooling cycles (GHSV ≈ 480'000 h^{-1}). For methane steam reforming tests, an oxidative pretreatment at 1173 K under 0.1% CH_4, 1% O_2, 5% H_2O, 5% CO_2 in N_2 was performed before reaction, then oxygen was removed and 0.15% CO was added to the gas feed (λ=0.99). Reactants and products were analyzed with a MKS MultiGas 2030 FTIR Continuous Gas Analyzer. Three consecutive heating/cooling cycles up to 1173 K were carried out to reach stable behavior.

2.4. Monolith samples activity tests. Catalytic tests on washcoated catalyst monoliths were performed by inserting a 0.70" D x 1.0" L sized core in a quartz tube and flowing the same reaction atmosphere as powder experiments, reaching a total GHSV of 19'000 h^{-1}. The space velocity was measured as the ratio between the gas flow (2 L/min) and the volume occupied by the coated core.

Monolith samples were tested degreened and after two established procedures for synthetic aging (2-modes or 4-modes). The 2-modes synthetic aging process consisted in holding the sample at 1223 K for 50 hours, repeating 60-second-long cycles of 54 s lean (4% O_2/10% H_2O) and 6 s rich pulses (3% CO/1% H_2/10% H_2O). The 4-modes procedure involved holding the coated core for 100 h at an effective temperature of 1183 K under 60 s cycles of stoichiometric, rich, and lean gas mixtures, with temperature spikes reaching over 1273 K. Methane conversion on degreened and aged samples was evaluated during three consecutive heating/cooling cycles from 373 K to 1173 K; the third cycle is reported in the following as representative of the stable catalytic behavior. Lambda sweep experiments were also carried out under synthetic gas composition by performing a series of individual light-off tests with different lambda levels. Gas composition was held constant for every lambda level (2000 ppm CH_4, 2000 ppm NO, 5000 ppm CO, 1667 ppm H_2, 5% CO_2, 5% H_2O, balance N_2) while O_2 was varied to achieve different λ (0.968 – 1.028) using a Horiba MEXA-730λ air-to-fuel ratio analyzer. The CH_4, CO and NO_x conversions were evaluated as function of temperature and the performance at 823 K was plotted against FG lambda setting to generate the lambda sweep performance.

3. RESULTS AND DISCUSSION

3.1. Characterization of Pd/CeO_2 powder catalysts. Surface area, average particle size and measured Pd loading of the catalytic samples prepared in this work are summarized in Table 1.

Table 1. BET surface area, average particle size and measured Pd loading of evaluated catalytic samples and support oxides.

Sample	BET surface area (m^2/g)	Measured Pd loading (wt.%)[a]	Average particle size (nm)[b]
Al_2O_3(873)	129.2	-	7
CeO_2(873)	78.8	-	10
CeO_2(1173)	23.4	-	25
CeO_2(1473)	3.8	-	53
1PdCe1173IW	19.6	0.93	28
1PdCe1173M	24.9	0.99	27
1PdCe1473M	5.2	1.01	50
4PdAl873IW	122.8	4.0	7
4PdCe873IW	69.8	4.0	10
4PdCe1173IW	14.6	3.94	26
4PdCe1173M	22.1	3.92	25
4PdCe1473M	3.1	4.03	57

a: measured by ICP-MS elemental analysis. b: calculated by using the Scherrer's equation.[39]

XRD profiles of CeO_2(1173), CeO_2(1473) and supported catalysts are reported in Figure 1. All samples display peaks corresponding to the ceria fluorite structure, which appear sharper on samples prepared on CeO_2(1473) (Figure 1A). This is a consequence of the higher calcination temperature of the ceria support, that results in larger particle size and lower surface area compared to CeO_2(1173), as reported in Table 1. Irrespective of the support oxide, on 1wt.% Pd catalysts no palladium peaks can be detected, suggesting a uniform dispersion of the noble metal on the ceria

surface (Figure 1B). At 4wt.%Pd loading, only oxidized PdO is observed on PdCeIW while a combination of PdO and Pd can be noticed on the samples prepared by milling on CeO_2(1473) and, to a lesser extent, on CeO_2(1173).

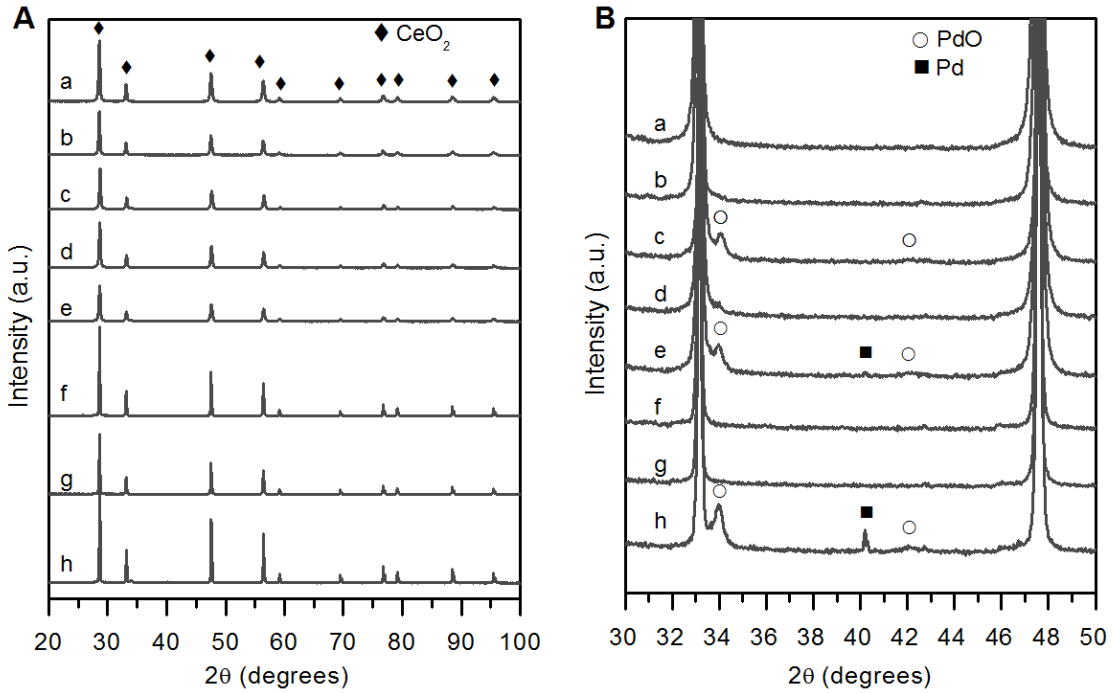

Figure 1. XRD patterns (A) with focus on the Pd-PdO range (B) of: a) CeO_2(1173), b) 1PdCe1173IW, c) 4PdCe1173IW, d) 1PdCe1173M, e) 4PdCe1173M, f) CeO_2(1473), g) 1PdCe1473M, h) 4PdCe1473M. Samples were characterized after 2 methane oxidation cycles up to 1173 K.

Morphological characterization by HRTEM of reference samples prepared by incipient wetness, reported in our previous works, revealed the presence of palladium particles of ca. 1-4 nm in size uniformly dispersed on the ceria surface.[38] Conversely, the milled samples were characterized by a peculiar amorphous shell on a ceria crystalline core structure, reported as responsible for an enhanced methane oxidation activity.[35] The shell structure is observed also here on 4PdCe1473M, despite the high palladium loading and low surface area. On this sample, low magnification HRTEM images reported in Figure 2A-B show aggregates of large ceria particles, their size ranging from ca. 10 up to 100 nm. Their thickness hinders a proper analysis by TEM, as only a

few crystallites are thin enough to get lattice fringes. These ceria particles are considered representative of the whole sample, showing well-defined geometrical features as a consequence of the high calcination temperature as well as the characteristic rounded edges.[35] The area enclosed in the black square in Figure 2B is shown under HRTEM mode in Figure 2C. Ceria crystallites oriented along the [110] crystallographic direction are clearly visible with lattice fringes at 3.12 and 2.71 Å corresponding to the (111) and (200) planes, respectively. At the surface of the ceria crystallites small clusters are observed, marked by arrows in Figure 2C-E, extraordinarily well-dispersed over the entire sample and measuring less than 0.5 nm in size. Their small size hinders lattice fringes analysis but their darker shade and previous studies suggest they are likely comprised of palladium.[38] These clusters appear to occupy defect sites, as shown in Figure 2C, inset "a". The area enclosed in the black square of Figure 2E is shown at higher magnification in Figure 2F, highlighting the existence of a thin amorphous layer covering the ceria surface (marked by lines between arrows) in addition to the sub-nanometric clusters.

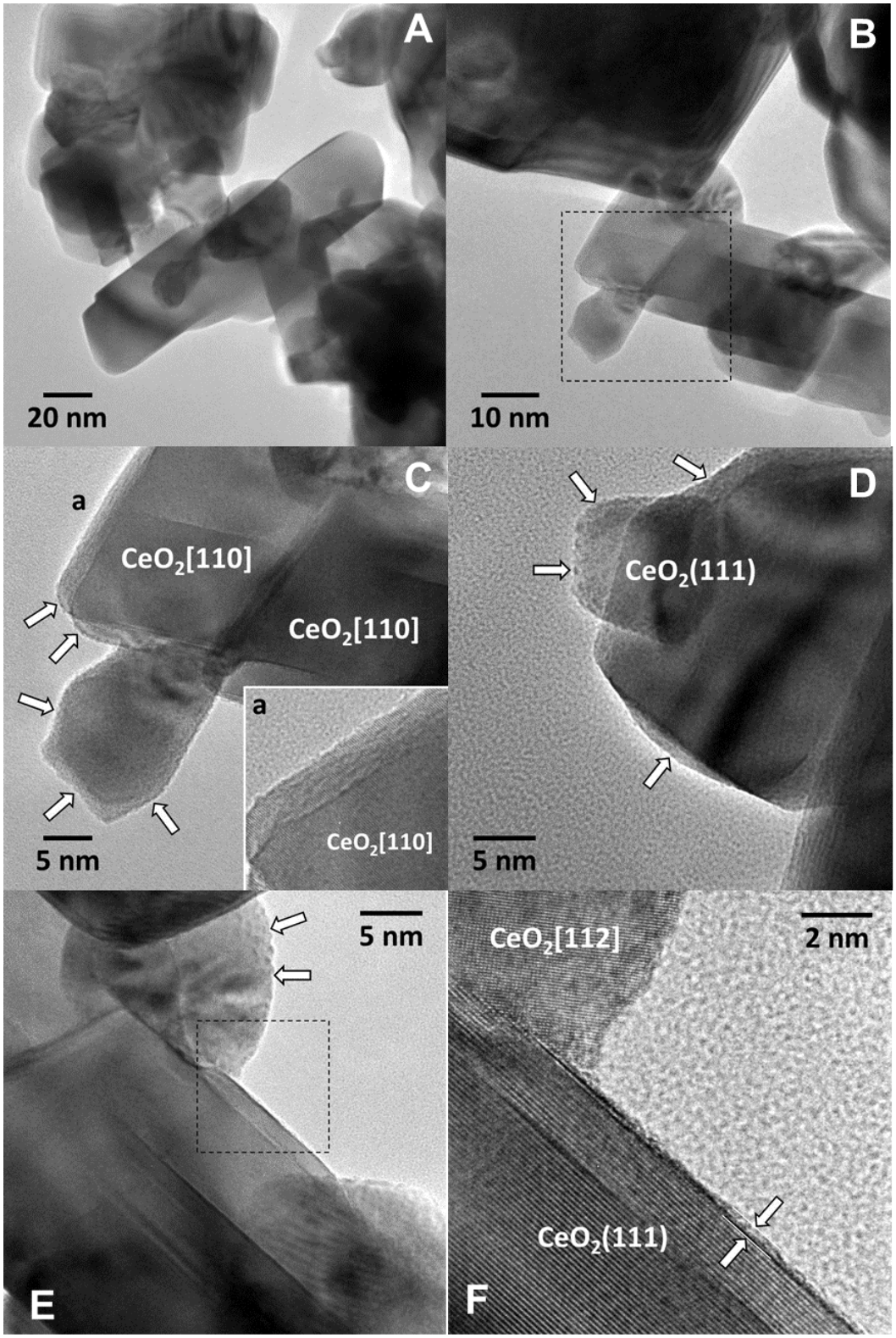

Figure 2. HRTEM images in low (A,B) and high (C-F) magnification of 4PdCe1473M after two reaction cycles up to 1173 K.

The redox properties of supported palladium species were investigated by the analysis of the oxygen release and uptake profiles recorded during temperature programmed oxidation (TPO) experiments. Oxygen profiles of the 3rd heating/cooling cycle, representative of the stable Pd behavior, are shown in Figure 3. On samples prepared by incipient wetness impregnation the main oxygen release peak is centered at around 1060 K, which is attributed to bulk PdO decomposition[40] in agreement with PdO particles dispersed on the ceria surface identified by TEM characterization.[38] Conversely, samples prepared by milling exhibit a more complex profile, displaying multiple O_2 release peaks with a larger contribution at high temperature (indicated with an asterisk in Figure 3), thus suggesting the presence of oxidized Pd species in stronger interaction with ceria. An exception is represented by the 1PdCe1173M sample, which is characterized by a major oxygen release peak at low temperature (ca. at 1000 K) and a lesser amount of O_2 exchanged, as highlighted by the quantitative analysis of oxygen release and uptake reported in Table S1 for all samples. These differences hint at a lower interaction between palladium and ceria on this sample, possibly leading to poorer methane oxidation performance.

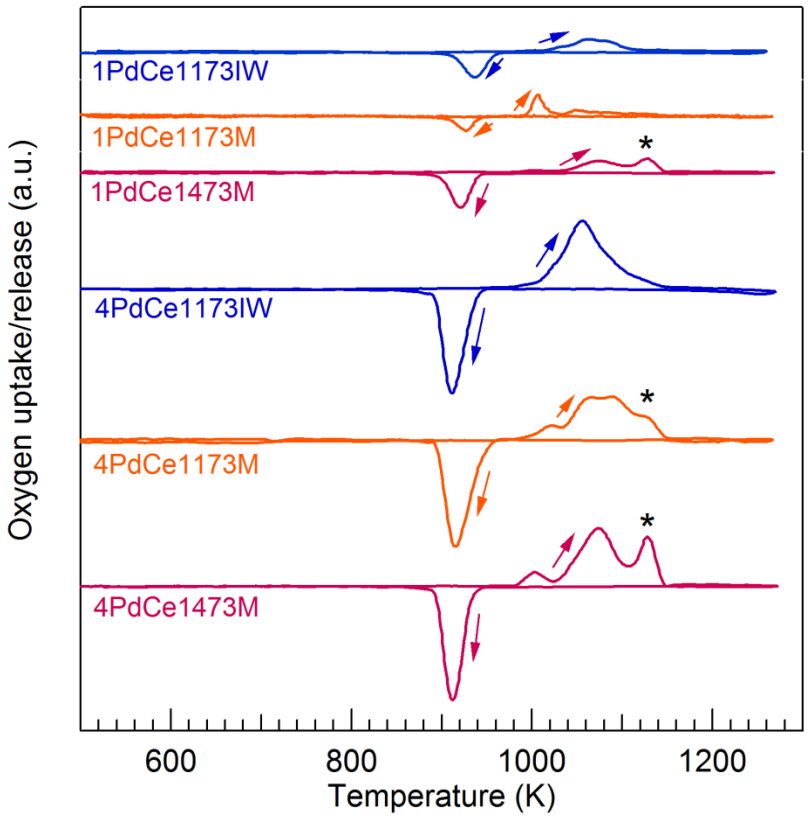

Figure 3. Oxygen profiles of 1wt.% and 4wt.%Pd/CeO_2 samples recorded during TPO experiments, 3rd heating/cooling cycle. High temperature oxygen release peak is highlighted by an asterisk.

3.2. Catalytic activity of powder samples. A first evaluation of the best performing Pd/CeO_2 samples was carried out by testing 1wt.% Pd/CeO_2 catalysts prepared by incipient wetness impregnation (1PdCe1173IW) and by dry mechano-chemical synthesis using commercial ceria with high thermal stability, calcined at 1173 K and 1473 K prior to synthesis (1PdCe1173M and 1PdCe1473M, respectively).

The methane conversion curves recorded at high space velocity (≈480'000 h^{-1}) reported in Figure 4 clearly point out that the highest methane oxidation activity is obtained by 1PdCe1473M. Indeed, as reported in our previous work,[36] the combination of $Pd(OAc)_2$ milled on low surface area ceria

(calcined at 1473 K, ~4 m^2/g surface area) simultaneously ensures low temperature methane activation and a negligible activity drop at temperatures above 900 K. This was attributed to a specific Pd^0/Pd^{2+} arrangement stabilized on the ceria surface, promoting surface oxygen mobility and resulting in higher methane oxidation reaction rate compared to IW samples where Pd^{2+}/Pd^{4+} in addition to low amounts of Pd^0 species were found by AP-XPS.[38] The trend confirms the results of activity tests performed under ideal reaction conditions and lower space velocity (0.5% CH_4, 2% O_2 in He, GHSV≈180'000 h^{-1}, Figure S1).

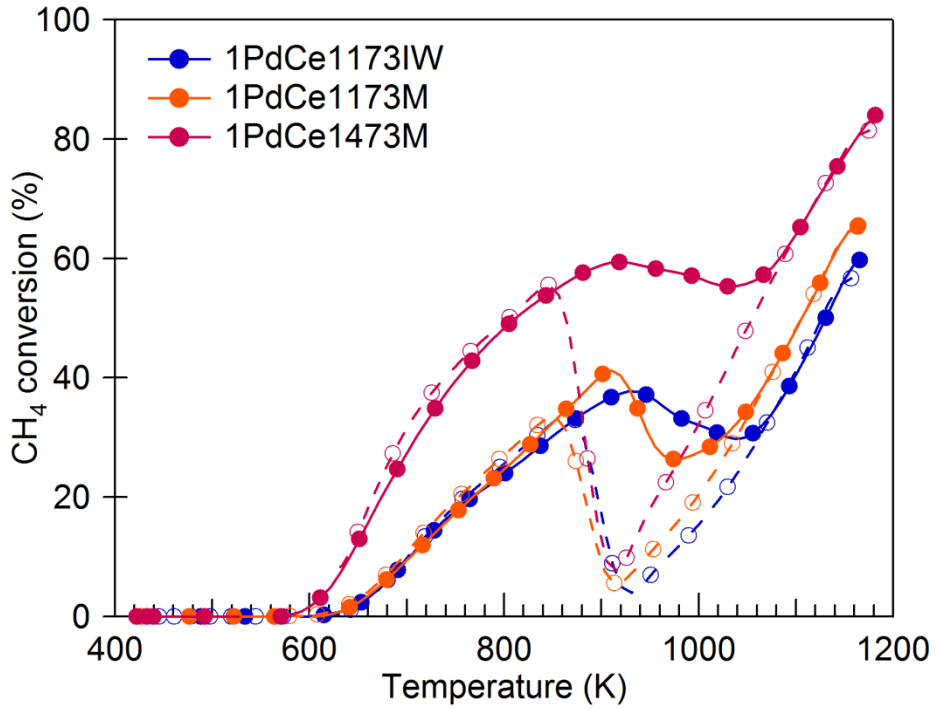

Figure 4. Methane oxidation activity of 1wt.%Pd/CeO_2 samples at GHSV≈480'000 h^{-1}. Solid line, full symbols: heating; dashed line, open symbols: cooling.

Methane steam reforming experiments confirm the improved performance of the milled sample compared to the sample prepared by the commercial wet synthesis. Methane conversion curves reported in Figure 5 show the 1PdCe1173M milled sample outperforms the reference IW sample,

displaying superior methane conversion during both heating and cooling ramps (by ca. 10-15%) and methane activation at lower temperature (below 600 K).

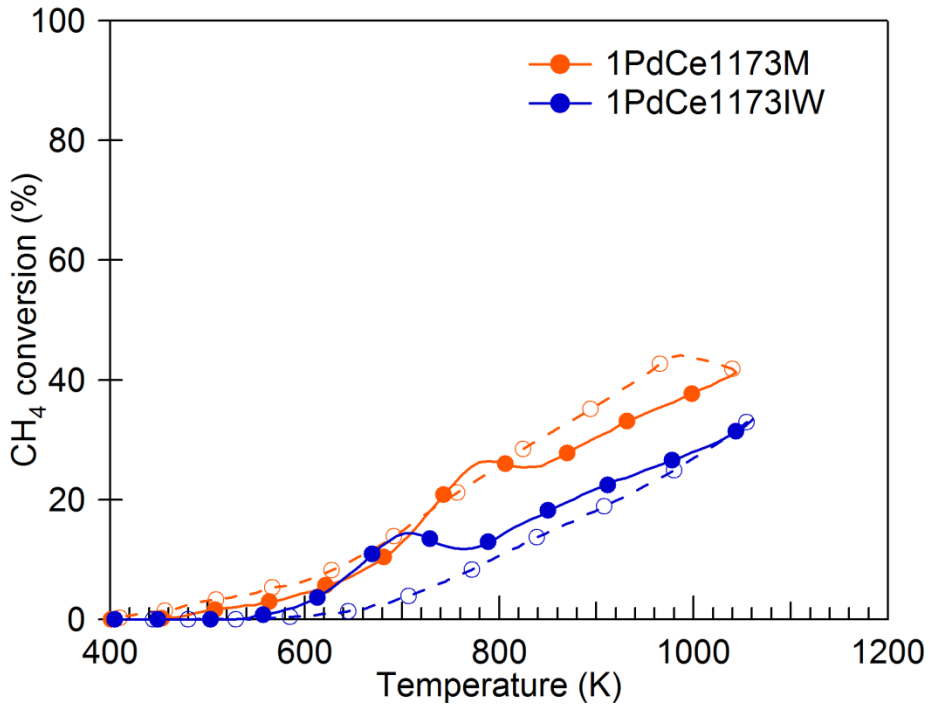

Figure 5. Steam reforming activity of 1wt.%Pd/CeO_2(1173) samples (GHSV≈480'000 h^{-1}). Solid line, full symbols: heating; dashed line, open symbols: cooling.

Nevertheless, both steam reforming (Figure 5) and oxidation tests (Figure 4) highlight that 1wt.% Pd samples are not able to reach full methane conversion at high space velocity (480'000 h^{-1}), a condition required to be able to comply to the current legislation limits at tailpipe. Consequently, aiming at achieving full methane conversion, a corresponding series of 4wt.%Pd/CeO_2 samples (4PdCe873IW, 4PdCe1173IW, 4PdCe1173M, 4PdCe1473M) was prepared and evaluated for methane oxidation. The light-off curves are reported in Figure 6, where the sample prepared by dry milling $Pd(OAc)_2$ on ceria calcined at 1473 K prior to synthesis

(4PdCe1473M) showed the highest activity and reached 95% conversion at 860 K, while samples prepared on higher surface area ceria displayed lower activity.

Further oxidation tests clearly showed that the 4PdCe1473M sample also outperformed a reference sample prepared on alumina calcined at 873 K, as well as a fully formulated TWC (Figure 7). The 4PdAl873IW sample displayed lower light-off temperatures compared to the milled 4PdCe1473M, but on this sample the activity undergoes a severe drop during cooling and it is not recovered until 700 K, which is typical of alumina-supported Pd catalysts.[41–43] This behavior is especially undesirable on TWC applications, as the activity loss during cooling accounts for unburned methane release during operation. In fact, in real-life applications the operating temperature depends on the engine regime conditions, hence the cooling process to 700 K cannot be controlled and on Al_2O_3-based catalysts it might result in prolonged release of large amounts of CH_4, above legislation limits. The ceria capacity to reduce this loss by promoting Pd re-oxidation during cooling and thus exhibiting a higher methane conversion averaged on the whole temperature range is much more favorable for methane abatement applications.[44–47]

Moreover, methane oxidation stability tests carried out at 723 K in excess steam (10 vol% H_2O added to the gas feed) on 1wt.% and 4wt.%Pd samples (Figure S2) show that milled catalysts are less deactivated in the 24-hour period and retain a higher conversion value in isothermal conditions compared to samples prepared by incipient wetness impregnation. These results indicated catalysts prepared by dry milling as promising materials and for this reason the 4PdCe1473M sample has been selected for evaluation of activity under conditions closer to final application.

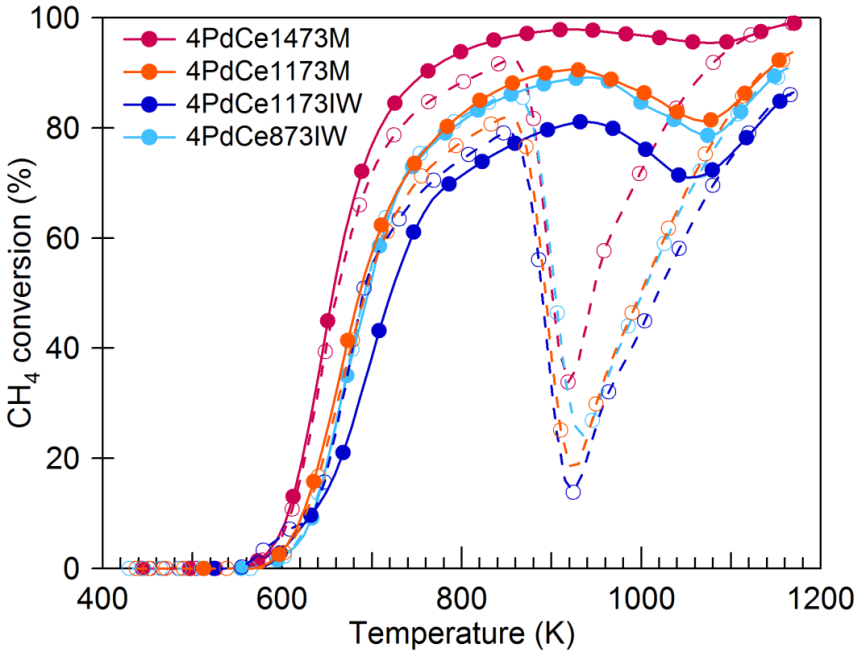

Figure 6. Methane oxidation activity of 4 wt.% Pd/CeO_2 samples (GHSV≈480'000 h^{-1}). Solid line, full symbols: heating; dashed line, open symbols: cooling.

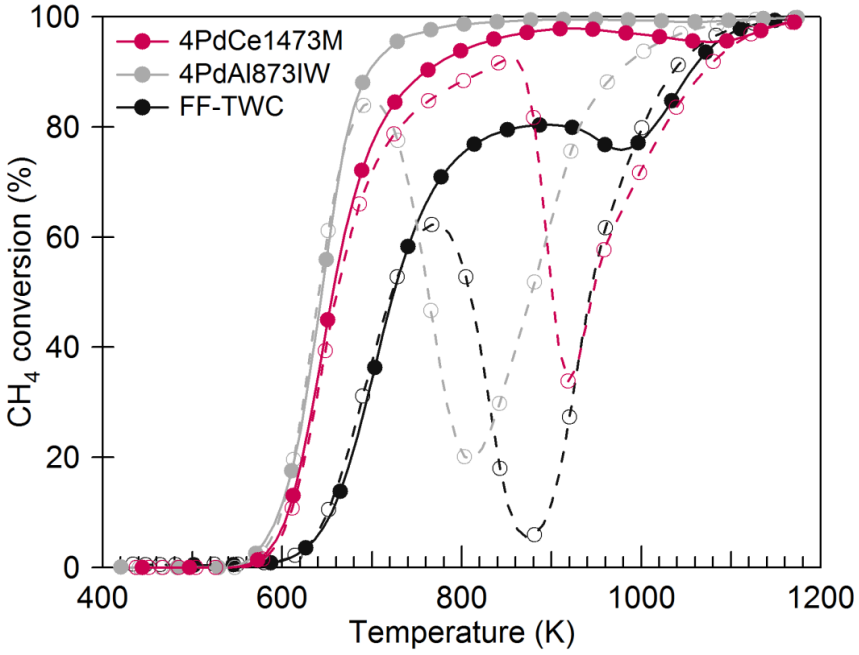

Figure 7. Methane oxidation activity of 4PdCe1473M compared to 4PdAl873IW and FF-TWC (GHSV≈480'000 h^{-1}). Solid line, full symbols: heating; dashed line, open symbols: cooling.

3.3. Catalytic activity of monolith samples. As the 4PdCe1473M sample exhibited remarkable performance in powder form, further testing was carried out on the milled sample coated on a

cordierite core. Due to the larger amount of catalytic powder needed for industrial lab-scale washcoating process, the dry mechano-chemical synthesis was scaled up from 1 g to 10 g using a planetary ball-mill instead of a vibratory mini-mill. The synthesis scale-up was not straightforward and comparative 4PdCe1473M samples did not exhibit fully coincident activity (Figure S3). While further studies could be conducted to optimize the scale-up synthesis, the relatively minor performance discrepancies observed allowed this sample to be considered representative and as such was used for washcoating and testing.

In addition, it is worth mentioning that the established process for cordierite cores washcoating involves dipping the cores into a slurry containing the Pd/CeO_2 catalytic powders and an alumina-based binder. Several dipping steps are usually performed to reach the desidered catalyst or noble metal loading, with low temperature calcination treatments (usually at 873 K) in air between each step. The coating process was not altered, possibly leading to a slight worsening in the catalytic activity exhibited by milled samples. Indeed, as reported in a previous work, an oxidizing pretreatment in air negatively affects the methane oxidation performance of Pd/CeO_2 milled samples.[36]

The activity of the 4PdCe1473M coated monolith was compared to reference 4PdCe873IW and 4PdAl873IW counterparts under methane oxidation and steam reforming conditions, before and after synthetic aging. The performance of degreened samples is shown in Figure 8a and 8c for methane oxidation and steam reforming, respectively. As already observed in tests carried out on samples in powder form, the degreened milled sample outperforms its 4PdCe873IW counterpart in lean methane oxidation (Figure 8a), while 4wt.%Pd supported on alumina onsets the reaction at lower temperatures (ca. 25 K) but displays a significant conversion loss during cooling. In rich steam reforming conditions (Figure 8c) all samples exhibit virtually identical activity. Under this

reducing atmosphere palladium is found mostly as Pd metal, consequently no hysteretic behavior is observed during reaction.

Catalysts were then aged under 2-modes conditions (50 hours at 1223 K), in order to verify the durability performance of evaluated catalysts.[48] After aging, the investigated samples exhibit noticeable differences in methane oxidation performance (Figure 8b), with the milled sample displaying the worst catalytic activity and suffering a 80 K shift to higher light-off temperatures compared to its degreened conditions. A similar effect is observed under steam reforming conditions (Figure 8d).

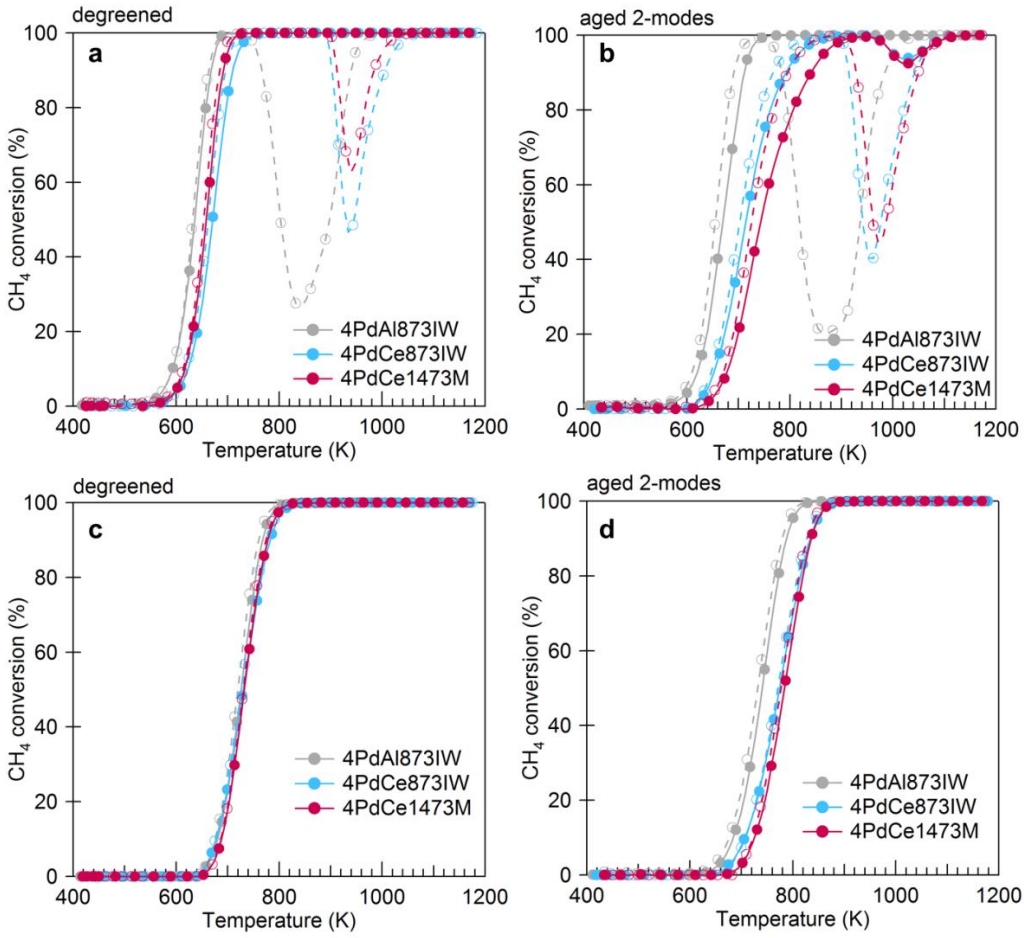

Figure 8. Catalytic activity in methane oxidation (a,b) and methane steam reforming (c,d) of 4PdCe1473M, 4PdCe873IW and 4PdAl873IW on monolith cores. (a,c) degreened samples; (b,d) after 2-modes aging (1223 K, 50 h). Solid line, full symbols: heating; dashed line, open symbols: cooling.

The 4PdCe1473M catalysts in the fresh and aged coated monoliths were studied by TEM after scratching the interior of various channels (Figure 9). As expected from the washcoating procedure, a mixture of Pd/CeO_2 and Al_2O_3 particles were identified in all cases. The alumina binding particles exhibited a crystallite size of about 10-15 nm whereas CeO_2 particles in the fresh sample measured between 30 and 150 nm (Figure 9A). Under high magnification, the fresh sample showed the occurrence of well-dispersed, subnanometric structures, which were ascribed to Pd in strong contact with the ceria support (marked by red circles in Figure 9B), as in the powdered sample. In contrast, in the aged sample the ceria crystallites appeared strongly sintered and ranged mostly from 100 up to 300 nm in size (Figure 9C). The HRTEM study was difficult due to the thickness of the ceria crystallites and it was not possible to identify subnanometric structures. Nevertheless, larger Pd particles were identified by EDX (Figure 9D), which were not present in the fresh sample. These Pd particles measured about 2-4 nm. No Pd particles were encountered on Al_2O_3, indicating that no Pd migration occurred from ceria to alumina under aging conditions. Therefore, the loss of catalytic activity in the aged coated monolith is ascribed to the sintering of both Pd phase and CeO_2 support.

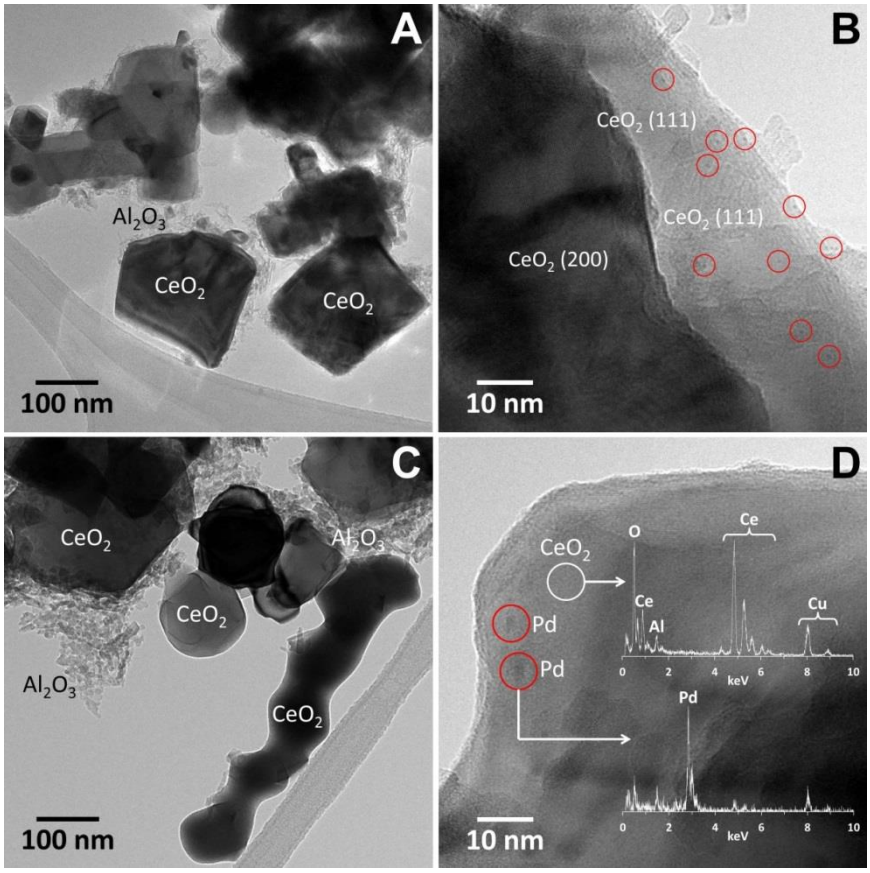

Figure 9. HRTEM of fresh (A,B) and aged (C,D) 4PdCe1473M coated monoliths.

3.4. Lambda sweep evaluation

To evaluate the performance of the prepared sample as a function of the air-to-fuel ratio, the 2-modes aged milled catalyst was tested under synthetic gas composition at different λ (0.968 – 1.028) and the CH_4, CO and NO_x conversions were evaluated as a function of temperature. The lambda sweep was evaluated at 823 K and compared to the FF-TWC after 4-modes aging, as shown in Figure 10. It can be clearly observed that, unlike TWC for gasoline engines,[17] the optimum λ is found in the rich region for methane abatement TWC. In fact, the highest conversion for simultaneous NO_x reduction and CO and CH_4 oxidation is found at around λ = 0.98. This confirms previous findings[20,21] and further suggests that methane steam reforming is an effective

methane abatement mechanism in three-way catalyst applications above 773 K; on the other hand, working in the rich region entails a higher fuel consumption, possibly leading to a lower CO_2 benefit of NG compared to gasoline. Moreover, the Pd-PdO transition between rich and lean feed appears to play a key role in the CH_4 conversion loss around the stoichiometric λ, thus suggesting that future research may be focused on this transient behavior to optimize catalyst performance and to shift the optimum working range towards the stoichiometric or lean regime.

The difference in performance between the 4PdCe1473M milled sample and the FF-TWC might be ascribed to their different formulations. Despite both samples being characterized by a high total PGM loading, in the FF-TWC there is a large amount of Rh (20 g/ft^3, 10% Rh of the total PGM) which largely contributes to the better performance of the FF-TWC at the richer conditions and significantly affects its catalytic light-off behavior (Figure S4), while the milled sample contains only Pd. Nonetheless, the sample prepared by dry milling displays comparable catalytic activity in the whole evaluated λ range, hence exhibiting a promising performance for real-life applications.

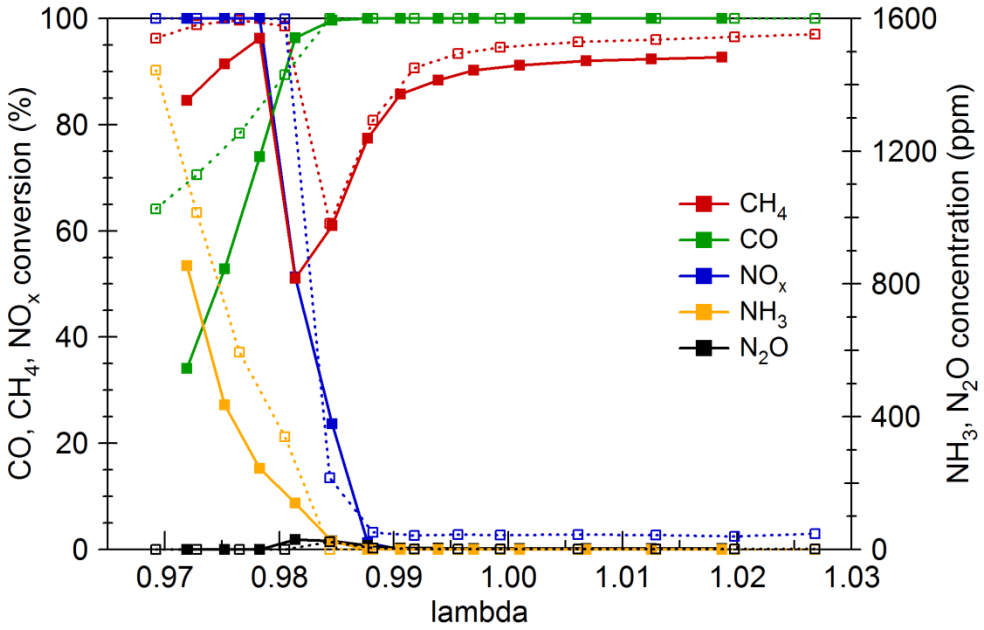

Figure 10. Synthetic reactor results with full gas mixture at 823 K for the 2-modes aged 4PdCe1473M sample (solid line, full symbols) and the 4-modes aged FF-TWC (dotted line, open symbols).

4. CONCLUSIONS

Reactivity tests carried out in a more complex gas mixture under lean and rich conditions confirmed previous findings reporting higher reactivity on Pd/CeO_2 samples prepared by dry mechano-chemical synthesis compared to incipient wetness impregnation.[38] Remarkably, sample 4PdCe1473M, prepared by milling palladium acetate nanopowders on a low surface area ceria (~4 m^2/g, calcined at 1473 K prior to synthesis), achieved almost full methane conversion (above 95%) at high space velocity testing conditions (480'000 h^{-1} GHSV) under a gas mixture containing CO, CO_2 and H_2O, which are known to inhibit methane oxidation[13,14] and are always present in large quantities in NGVs exhausts.[20]

When washcoated on a monolith core, the 4PdCe1473M sample retained its catalytic performance, showing improved methane oxidation activity compared to other reference samples

supported on commercial ceria and on commercial alumina with higher surface area. Under steam reforming conditions all fresh samples exhibited similar activity, suggesting that the peculiar Pd-Ce surface arrangement of 4PdCe1473M plays a less significant role under a CH_4+H_2O atmosphere. In addition, established aging procedures resulted in significant deactivation of the milled sample. It is possible that the evaluated catalyst is affected to a greater extent by aging under a rich/lean oscillating regime compared to the conventional IW samples, but a negative effect of the washcoating process cannot be excluded; catalytic performance of 4PdCe1473M might be influenced by the preparation and coating process, which involves a series of oxidative steps shown to be detrimental for these catalytic materials.[36] An optimized washcoating procedure should be appropriately tuned for this catalytic system. Nevertheless, improving the aging resistance of the milled samples would be necessary for the sample preparation technique to have practical importance.

The evaluation of the simultaneous CH_4, CO and NO_x abatement as a function of λ confirmed the optimum working range of NGVs three-way catalysts to be in the rich region.[21] These results, coupled with the transient light-off experiments, indicate steam reforming as a promising methane abatement mechanism in TWC applications at high temperatures while methane oxidation remains the most active route for low temperature CH_4 abatement. Consequently, despite the high total PGM loading, which largely contributes to the cost of the aftertreatment system, and the contradicting results displayed by fresh and aged milled catalysts, the preparation of materials by dry mechano-chemical synthesis is worth further investigation, as it results in higher catalytic performance, especially at low temperature, while enabling a reduction of the solvent and energy requirements for catalysts production. To ensure a sustainable NGV aftertreatment system, the environmental impact advantage provided by the alternative synthesis procedure should be further

integrated by a reduction in the noble metal loading and by the shift of the TWC working range towards the lean region to reduce additional NG consumption.

NOTICE AND DISCLAIMER

While this article is believed to contain correct information, Ford Motor Company (Ford) does not expressly or impliedly warrant, nor assume any responsibility, for the accuracy, completeness, or usefulness of any information, apparatus, product, or process disclosed, nor represent that its use would not infringe the rights of third parties. Reference to any commercial product or process does not constitute its endorsement. This article does not provide financial, safety, medical, consumer product, or public policy advice or recommendation. Readers should independently replicate all experiments, calculations, and results. The views and opinions expressed are of the authors and do not necessarily reflect those of Ford. This disclaimer may not be removed, altered, superseded or modified without prior Ford permission.

ACKNOWLEDGMENTS

This work has been funded by Ford Motor Company under 2014-2195R University Research Program Award. MD acknowledges Regione Friuli Venezia Giulia for funding PhD under Operating Program of the European Social Fund 2014/2020. JL is a Serra Húnter Fellow and is grateful to ICREA Academia program and projects MICINN/FEDER RTI2018-093996-B-C31 and GC 2017 SGR 128.

REFERENCES

(1) Chen, H.; He, J.; Zhong, X. Engine Combustion and Emission Fuelled with Natural Gas: A Review. *Journal of the Energy Institute* **2019**, *92* (4), 1123–1136. https://doi.org/10.1016/j.joei.2018.06.005.

(2) Peterson, M. B.; Barter, G. E.; West, T. H.; Manley, D. K. A Parametric Study of Light-Duty Natural Gas Vehicle Competitiveness in the United States through 2050. *Applied Energy* **2014**, *125*, 206–217. https://doi.org/10.1016/j.apenergy.2014.03.062.

(3) Engerer, H.; Horn, M. Natural Gas Vehicles: An Option for Europe. *Energy Policy* **2010**, *38* (2), 1017–1029. https://doi.org/10.1016/j.enpol.2009.10.054.

(4) Yeh, S. An Empirical Analysis on the Adoption of Alternative Fuel Vehicles: The Case of Natural Gas Vehicles. *Energy Policy* **2007**, *35* (11), 5865–5875. https://doi.org/10.1016/j.enpol.2007.06.012.

(5) Raj, A. Methane Emission Control. *Johnson Matthey Technology Review* **2016**, *60* (4), 228–235. https://doi.org/10.1595/205651316X692554.

(6) Han, J. W.; Mintz, M.; Wang, M. *Waste-to-Wheel Analysis of Anaerobic-Digestion-Based Renewable Natural Gas Pathways with the GREET Model*; ANL/ESD/11-6; Argonne National Laboratory, 2011; p 40.

(7) Korakianitis, T.; Namasivayam, A. M.; Crookes, R. J. Natural-Gas Fueled Spark-Ignition (SI) and Compression-Ignition (CI) Engine Performance and Emissions. *Progress in Energy and Combustion Science* **2011**, *37* (1), 89–112. https://doi.org/10.1016/j.pecs.2010.04.002.

(8) Moore, C. W.; Zielinska, B.; Pétron, G.; Jackson, R. B. Air Impacts of Increased Natural Gas Acquisition, Processing, and Use: A Critical Review. *Environ. Sci. Technol.* **2014**, *48* (15), 8349–8359. https://doi.org/10.1021/es4053472.

(9) Camuzeaux, J. R.; Alvarez, R. A.; Brooks, S. A.; Browne, J. B.; Sterner, T. Influence of Methane Emissions and Vehicle Efficiency on the Climate Implications of Heavy-Duty Natural Gas Trucks. *Environmental Science & Technology* **2015**, *49* (11), 6402–6410. https://doi.org/10.1021/acs.est.5b00412.

(10) Clark, N. N.; McKain, D. L.; Johnson, D. R.; Wayne, W. S.; Li, H.; Akkerman, V.; Sandoval, C.; Covington, A. N.; Mongold, R. A.; Hailer, J. T.; Ugarte, O. J. Pump-to-Wheels Methane Emissions from the Heavy-Duty Transportation Sector. *Environ. Sci. Technol.* **2017**, *51* (2), 968–976. https://doi.org/10.1021/acs.est.5b06059.

(11) Geels, F.; Turnheim, B.; Asquith, M.; Kern, F.; Kivimaa, P.; European Environment Agency. *Sustainability Transitions: Policy and Practice.*; EEA Report 09/2019; Publications Office of the European Union: Luxembourg, 2019.

(12) *Commission Regulation (EU) No 582/2011 of 25 May 2011 Implementing and Amending Regulation (EC) No 595/2009 of the European Parliament and of the Council with Respect to Emissions from Heavy Duty Vehicles (Euro VI) and Amending Annexes I and III to Directive 2007/46/EC of the European Parliament and of the CouncilText with EEA Relevance*; 2011; p 168.

(13) Persson, K.; Pfefferle, L. D.; Schwartz, W.; Ersson, A.; Järås, S. G. Stability of Palladium-Based Catalysts during Catalytic Combustion of Methane: The Influence of Water. *Applied Catalysis B: Environmental* **2007**, *74* (3–4), 242–250. https://doi.org/10.1016/j.apcatb.2007.02.015.

(14) Gholami, R.; Alyani, M.; Smith, K. Deactivation of Pd Catalysts by Water during Low Temperature Methane Oxidation Relevant to Natural Gas Vehicle Converters. *Catalysts* **2015**, *5* (2), 561–594. https://doi.org/10.3390/catal5020561.
(15) Huang, W.; Goodman, E. D.; Losch, P.; Cargnello, M. Deconvoluting Transient Water Effects on the Activity of Pd Methane Combustion Catalysts. *Industrial & Engineering Chemistry Research* **2018**, *57* (31), 10261–10268. https://doi.org/10.1021/acs.iecr.8b01915.
(16) Einewall, P.; Tunestål, P.; Johansson, B. Lean Burn Natural Gas Operation vs. Stoichiometric Operation with EGR and a Three Way Catalyst. *SAE Special Publications* **2005**, *Vol.2005*, 343–362. https://doi.org/10.4271/2005-01-0250.
(17) Heck, R. M.; Farrauto, R. J.; Gulati, S. T. *Catalytic Air Pollution Control: Commercial Technology*, 3rd ed.; John Wiley & Sons, 2012.
(18) Farrauto, R. J.; Deeba, M.; Alerasool, S. Gasoline Automobile Catalysis and Its Historical Journey to Cleaner Air. *Nat Catal* **2019**, *2* (7), 603–613. https://doi.org/10.1038/s41929-019-0312-9.
(19) Matam, S. K.; Chiarello, G. L.; Lu, Y.; Weidenkaff, A.; Ferri, D. PdO_x/Pd at Work in a Model Three-Way Catalyst for Methane Abatement Monitored by Operando XANES. *Top Catal* **2013**, *56* (1–8), 239–242. https://doi.org/10.1007/s11244-013-9960-1.
(20) Xi, Y.; Ottinger, N.; Liu, Z. G. Development of a Lab Reactor System for the Evaluation of Aftertreatment Catalysts for Stoichiometric Natural Gas Engines. *SAE Technical Paper* **2017**, 2017-01–0999. https://doi.org/10.4271/2017-01-0999.
(21) Ferri, D.; Elsener, M.; Kröcher, O. Methane Oxidation over a Honeycomb Pd-Only Three-Way Catalyst under Static and Periodic Operation. *Applied Catalysis B: Environmental* **2018**, *220*, 67–77. https://doi.org/10.1016/j.apcatb.2017.07.070.
(22) Arosio, F.; Colussi, S.; Trovarelli, A.; Groppi, G. Effect of Alternate CH_4-Reducing/Lean Combustion Treatments on the Reactivity of Fresh and S-Poisoned Pd/CeO_2/Al_2O_3 Catalysts. *Applied Catalysis B: Environmental* **2008**, *80* (3–4), 335–342. https://doi.org/10.1016/j.apcatb.2007.11.030.
(23) Fouladvand, S.; Schernich, S.; Libuda, J.; Grönbeck, H.; Pingel, T.; Olsson, E.; Skoglundh, M.; Carlsson, P.-A. Methane Oxidation Over Pd Supported on Ceria–Alumina Under Rich/Lean Cycling Conditions. *Topics in Catalysis* **2013**, *56* (1–8), 410–415. https://doi.org/10.1007/s11244-013-9988-2.
(24) Bounechada, D.; Groppi, G.; Forzatti, P.; Kallinen, K.; Kinnunen, T. Effect of Periodic Lean/Rich Switch on Methane Conversion over a Ce–Zr Promoted Pd-Rh/Al_2O_3 Catalyst in the Exhausts of Natural Gas Vehicles. *Applied Catalysis B: Environmental* **2012**, *119–120*, 91–99. https://doi.org/10.1016/j.apcatb.2012.02.025.
(25) Hellman, A.; Resta, A.; Martin, N. M.; Gustafson, J.; Trinchero, A.; Carlsson, P.-A.; Balmes, O.; Felici, R.; van Rijn, R.; Frenken, J. W. M.; Andersen, J. N.; Lundgren, E.; Grönbeck, H. The Active Phase of Palladium during Methane Oxidation. *J. Phys. Chem. Lett.* **2012**, *3* (6), 678–682. https://doi.org/10.1021/jz300069s.
(26) Huang, F.; Chen, J.; Hu, W.; Li, G.; Wu, Y.; Yuan, S.; Zhong, L.; Chen, Y. Pd or PdO: Catalytic Active Site of Methane Oxidation Operated Close to Stoichiometric Air-to-Fuel for Natural Gas Vehicles. *Applied Catalysis B: Environmental* **2017**, *219*, 73–81. https://doi.org/10.1016/j.apcatb.2017.07.037.
(27) Nilsson, J.; Carlsson, P.-A.; Martin, N. M.; Adams, E. C.; Agostini, G.; Grönbeck, H.; Skoglundh, M. Methane Oxidation over Pd/Al_2O_3 under Rich/Lean Cycling Followed by

Operando XAFS and Modulation Excitation Spectroscopy. *Journal of Catalysis* **2017**, *356*, 237–245. https://doi.org/10.1016/j.jcat.2017.10.018.
(28) Zanoletti, M.; Klvana, D.; Kirchnerova, J.; Perrier, M. Modeling of Autocyclic Reactor for the Removal of Unburned Methane from Emissions of Natural Gas Engines. *Ind. Eng. Chem. Res.* **2010**, *49* (3), 1063–1070. https://doi.org/10.1021/ie900701h.
(29) Wang, D.; Gong, J.; Luo, J.; Li, J.; Kamasamudram, K.; Currier, N.; Yezerets, A. Distinct Reaction Pathways of Methane Oxidation on Different Oxidation States over Pd-Based Three-Way Catalyst (TWC). *Applied Catalysis A: General* **2019**, *572*, 44–50. https://doi.org/10.1016/j.apcata.2018.12.022.
(30) Chen, J.; Wu, Y.; Hu, W.; Qu, P.; Zhang, G.; Granger, P.; Zhong, L.; Chen, Y. New Insights into the Role of Pd-Ce Interface for Methane Activation on Monolithic Supported Pd Catalysts: A Step Forward the Development of Novel PGM Three-Way Catalysts for Natural Gas Fueled Engines. *Applied Catalysis B: Environmental* **2020**, *264*, 118475. https://doi.org/10.1016/j.apcatb.2019.118475.
(31) Senftle, T. P.; van Duin, A. C. T.; Janik, M. J. Methane Activation at the Pd/CeO_2 Interface. *ACS Catalysis* **2017**, *7* (1), 327–332. https://doi.org/10.1021/acscatal.6b02447.
(32) Su, Y.-Q.; Liu, J.-X.; Filot, I. A. W.; Zhang, L.; Hensen, E. J. M. Highly Active and Stable CH_4 Oxidation by Substitution of Ce^{4+} by Two Pd^{2+} Ions in CeO_2 (111). *ACS Catalysis* **2018**, *8* (7), 6552–6559. https://doi.org/10.1021/acscatal.8b01477.
(33) Li, C.; Li, W.; Chen, K.; Ogunbiyi, A. T.; Zhou, Z.; Duan, Q.; Xue, F. Highly Active Pd Catalysts Supported on Surface-Modified Cobalt-Nickel Mixed Oxides for Low Temperature Oxidation of Lean Methane. *Fuel* **2020**, *279*, 118372. https://doi.org/10.1016/j.fuel.2020.118372.
(34) Murata, K.; Kosuge, D.; Ohyama, J.; Mahara, Y.; Yamamoto, Y.; Arai, S.; Satsuma, A. Exploiting Metal–Support Interactions to Tune the Redox Properties of Supported Pd Catalysts for Methane Combustion. *ACS Catalysis* **2020**, *10* (2), 1381–1387. https://doi.org/10.1021/acscatal.9b04524.
(35) Danielis, M.; Colussi, S.; de Leitenburg, C.; Soler, L.; Llorca, J.; Trovarelli, A. Outstanding Methane Oxidation Performance of Palladium-Embedded Ceria Catalysts Prepared by a One-Step Dry Ball-Milling Method. *Angewandte Chemie International Edition* **2018**, *57* (32), 10212–10216. https://doi.org/10.1002/anie.201805929.
(36) Danielis, M.; Colussi, S.; de Leitenburg, C.; Trovarelli, A. The Role of Palladium Salt Precursors in $Pd\text{-}PdO/CeO_2$ Catalysts Prepared by Dry Milling for Methane Oxidation. *Catalysis Communications* **2020**, *135*, 105899. https://doi.org/10.1016/j.catcom.2019.105899.
(37) Danielis, M.; Colussi, S.; de Leitenburg, C.; Soler, L.; Llorca, J.; Trovarelli, A. The Effect of Milling Parameters on the Mechanochemical Synthesis of $Pd–CeO_2$ Methane Oxidation Catalysts. *Catal. Sci. Technol.* **2019**, *9* (16), 4232–4238. https://doi.org/10.1039/C9CY01098J.
(38) Danielis, M.; Betancourt, L. E.; Orozco, I.; Divins, N. J.; Llorca, J.; Rodríguez, J. A.; Senanayake, S. D.; Colussi, S.; Trovarelli, A. Methane Oxidation Activity and Nanoscale Characterization of Pd/CeO_2 Catalysts Prepared by Dry Milling Pd Acetate and Ceria. *Applied Catalysis B: Environmental* **2021**, *282*, 119567. https://doi.org/10.1016/j.apcatb.2020.119567.
(39) Jenkins, R.; Snyder, R. L. *Introduction to X-Ray Powder Diffractometry*; Wiley: New York, 1996.

(40) Colussi, S.; Trovarelli, A.; Vesselli, E.; Baraldi, A.; Comelli, G.; Groppi, G.; Llorca, J. Structure and Morphology of Pd/Al_2O3 and Pd/CeO_2/Al_2O_3 Combustion Catalysts in Pd–PdO Transformation Hysteresis. *Applied Catalysis A: General* **2010**, *390* (1–2), 1–10. https://doi.org/10.1016/j.apcata.2010.09.033.
(41) McCarty, J. G. Kinetics of PdO Combustion Catalysis. *Catalysis Today* **1995**, *26* (3–4), 283–293. https://doi.org/10.1016/0920-5861(95)00150-7.
(42) Datye, A. K.; Bravo, J.; Nelson, T. R.; Atanasova, P.; Lyubovsky, M.; Pfefferle, L. Catalyst Microstructure and Methane Oxidation Reactivity during the Pd↔PdO Transformation on Alumina Supports. *Applied Catalysis A: General* **2000**, *198* (1–2), 179–196. https://doi.org/10.1016/S0926-860X(99)00512-8.
(43) Miller, J. B.; Malatpure, M. Pd Catalysts for Total Oxidation of Methane: Support Effects. *Applied Catalysis A: General* **2015**, *495*, 54–62. https://doi.org/10.1016/j.apcata.2015.01.044.
(44) Farrauto, R. J.; Lampert, J. K.; Hobson, M. C.; Waterman, E. M. Thermal Decomposition and Reformation of PdO Catalysts; Support Effects. *Applied Catalysis B: Environmental* **1995**, *6* (3), 263–270. https://doi.org/10.1016/0926-3373(95)00015-1.
(45) Groppi, G.; Cristiani, C.; Lietti, L.; Ramella, C.; Valentini, M.; Forzatti, P. Effect of Ceria on Palladium Supported Catalysts for High Temperature Combustion of CH_4 under Lean Conditions. *Catalysis Today* **1999**, *50* (2), 399–412. https://doi.org/10.1016/S0920-5861(98)00518-5.
(46) Colussi, S.; Trovarelli, A.; Cristiani, C.; Lietti, L.; Groppi, G. The Influence of Ceria and Other Rare Earth Promoters on Palladium-Based Methane Combustion Catalysts. *Catalysis Today* **2012**, *180* (1), 124–130. https://doi.org/10.1016/j.cattod.2011.03.021.
(47) McCabe, R. W.; Trovarelli, A. Forty Years of Catalysis by Ceria: A Success Story. *Applied Catalysis B: Environmental* **2016**, *197*, 1. https://doi.org/10.1016/j.apcatb.2016.04.044.
(48) Maunula, T.; Kallinen, K.; Savimäki, A.; Wolff, T. Durability Evaluations and Rapid Ageing Methods in Commercial Emission Catalyst Development for Diesel, Natural Gas and Gasoline Applications. *Topics in Catalysis* **2016**, *59* (10–12), 1049–1053. https://doi.org/10.1007/s11244-016-0588-9.

TABLE OF CONTENTS